

## References

- <sup>1</sup> Burch, B. A., "Effects of Contamination on Spacecraft Surfaces Exposed to Rocket Exhausts," AEDC-TR-68-23, April 1968, ARO Inc., Tullahoma, Tenn.
- <sup>2</sup> Hill, D. W., Jr. and Smith, D. K., "Effects and Control of Contamination from a Scaled MOL Altitude Control Thruster in a Tangential Orientation," AEDC-TR-69-146, Oct. 1969, ARO Inc., Tullahoma, Tenn.
- <sup>3</sup> Borson, E. N. and Landsbaum, E. M., "A Review of Available Rocket Contamination Results," TR-0200(4250-20)-2, Dec. 1969, Aerospace Corp., El Segundo, Calif.
- <sup>4</sup> Valentine, R. S., Rossi, F. S., and Kromfey, R. K., "Fluid Dynamic Effects on Apollo Engine Pressure Spikes," *Journal of Spacecraft and Rockets*, Vol. 5, No. 1, Jan. 1968, pp. 31-35.
- <sup>5</sup> Christos, T. et al., "Combustion Characteristics of Condensed-Phase Hydrazine-Type Fuels with Nitrogen Tetroxide," *Journal of Spacecraft and Rockets*, Vol. 4, No. 9, Sept. 1967, pp. 1224-1229.
- <sup>6</sup> Perlee, H. E. et al., "Preignition Phenomena in Small A-50/NTD Pulsed Rocket Engines," *Journal of Spacecraft and Rockets*, Vol. 5, No. 2, Feb. 1968, pp. 233-235.
- <sup>7</sup> Mayer, S. W., Taylor, D., and Schieler, L., "Preignition Products from Propellants at Simulated High-Altitude Conditions," *Combustion Science and Technology*, Vol. 1, 1969, pp. 119-129.
- <sup>8</sup> Seamans, T. F. and Dawson, B. E., "Hyperbolic Ignition at Reduced Pressures," Rept. RMD 5809-Q1, 1966, Thiokol Chemical Corp.
- <sup>9</sup> Takimoto, H. H. and Denault, G. C., "Combustion Residues from  $N_2O_4$ -MMH Motors," TR-0066(5210-10)-1, Sept. 1969, Aerospace Corp., El Segundo, Calif.

## Approximate Far-Field Flow Description for a Nozzle Exhausting into a Vacuum

GEORGE F. GREENWALD\*

McDonnell Douglas Astronautics Company, McDonnell Douglas Corp., Huntington Beach, Calif.

### Nomenclature

- $A$  = area  
 $B$  = empirical factor defined by Eq. (2)  
 $d$  = diameter  
 $K$  = shaping constant defined by Eq. (13)  
 $M$  = Mach number  
 $n$  = shaping term exponent  
 $r$  = radial distance from nozzle  
 $\gamma$  = ratio of specific heats  
 $\theta$  = angle from nozzle axis to streamline  
 $\theta_m$  = limiting streamline angle  
 $\rho$  = density

### Subscripts and superscripts

- \* = nozzle throat conditions  
 $ch$  = chamber conditions  
 $o$  = axis conditions

### Introduction

APPROXIMATE calculation techniques for use in describing the flow pattern of gas exhausting through a nozzle into a vacuum can be useful when time and/or facilities do not

allow for use of more accurate method-of-characteristics solutions. In addition, as indicated by Hill and Draper,<sup>1</sup> the use of method-of-characteristics solutions at distances beyond a few hundred exit radii is often unsuccessful because of program limitations. A method for far-field approximation of the complete flowfield was sought which would be sufficiently accurate, at least for preliminary design, while providing rapid results by use of hand calculations. Initial assessment of the problem led to a solution which combined the technique developed by Sibulkin and Gallaher<sup>2</sup> for axial density decay with the suggestion of Albini<sup>3</sup> for Mach number angular distribution. The method was only moderately successful. However, significant improvement was achieved by the addition of a "shaping" term and the imposition of the continuity and momentum relationships on the flow.

### Initial Approximation

At large distances from the nozzle, the streamlines appear to be straight radial lines emanating from a common source. The mass flux,  $\rho u$ , therefore, varies as  $1/r^2$ . Since at large  $r$  the velocity is constant (equal to  $u_{max}$ ), the density varies inversely with the square of the distance from the nozzle. The density decay can, therefore, be expressed as

$$\rho_o/\rho_{ch} = B(d^*/r)^2 \quad (1)$$

where  $B$  is approximated by<sup>2</sup>

$$B \cong [5(1 - \cos\theta_m)]^{-1} \quad (2)$$

The Mach number angular distribution was expressed in Ref. 3 as

$$\lim_{r \rightarrow \infty} \left[ \frac{M_o}{M} \right] = \cos^{1/2} \left( \frac{\pi}{2} \frac{\theta}{\theta_m} \right) \quad (3)$$

Equations (1) and (2) together with the isentropic relation for  $\rho_o/\rho_{ch}$  result in the following expression for the axial Mach number

$$M_o = [2/(\gamma - 1)]^{1/2} \{ [5(r/d^*)^2(1 - \cos\theta_m)]^{\gamma-1} - 1 \}^{1/2} \quad (4)$$

In the far field, however,

$$[5(r/d^*)^2(1 - \cos\theta_m)]^{\gamma-1} \gg 1 \quad (5)$$

Therefore,

$$\lim_{r \rightarrow \infty} [M_o] = [2/(\gamma - 1)]^{1/2} [5(1 - \cos\theta_m)]^{(\gamma-1)/2} (r/d^*)^{\gamma-1} \quad (6)$$

The complete Mach field can be defined by combining Eqs.

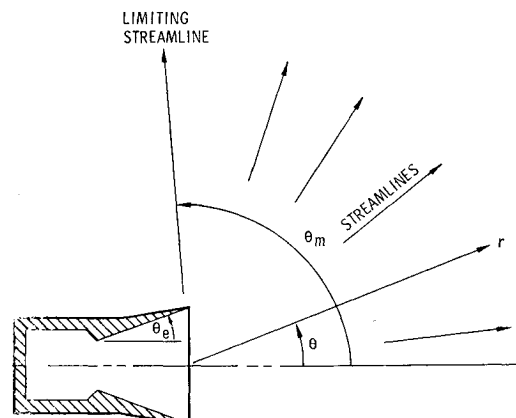


Fig. 1 Schematic representation of a nozzle exhausting into a vacuum.

Received July 20, 1970. This Note is based in part on work performed by the McDonnell Douglas Astronautics Company—Western Division under contract to the Air Force (F04701-69-C-0039).

\* Senior Engineer Scientist, Delta/MLV Aero/Thermodynamics Section, Flight Mechanics Department Development Engineering. Member AIAA.

(3) and (6)

$$M = \frac{M_o}{\cos^{1/2} \left( \frac{\pi}{2} \frac{\theta}{\theta_m} \right)} = \left\{ \frac{2[5(1 - \cos \theta_m)]^{\gamma-1}}{(\gamma - 1) \cos \left( \frac{\pi}{2} \frac{\theta}{\theta_m} \right)} \right\}^{1/2} \left( \frac{r}{d^*} \right)^{\gamma-1} \quad (7)$$

Equation (7) represents an approximation to the flow that is certainly amenable to rapid calculation techniques. However, the inaccuracies of the empirical relations expressed by Eqs. (2) and (3) are inherent to Eq. (7).

Figure 1 illustrates the appropriate nozzle coordinates, and Fig. 2 shows, for a typical axisymmetric nozzle, a comparison of the results obtained by Eq. (7) and a solution by method-of-characteristics. The combined approximations yield results which are only moderately successful in predicting the far-field plume characteristics.

### Improved Approximation

A more exact and reasonable approximation was developed by imposing the relationship (obtained from continuity and one-dimensional momentum) between area ratio and Mach number on the integral of the constant property contours. This modification, however, involved introduction of one additional empirical constant.

Equation (7) was modified by the addition of a shaping term, initially having two unspecified constants,  $K$  and  $n$

$$M = \{M_o / \cos^{1/2}[(\pi/2) \theta / \theta_m]\} + KM_o \sin^n[(\pi/2) \theta / \theta_m] \quad (8)$$

It will be shown that only one of the two constants is arbitrary. Specifying the axial Mach number  $M_o$  as in Eq. (6), combining with Eq. (8), and rearranging results in an expression for  $r$  in terms of  $M$  and  $\theta$

$$r = \{d^* M^{1/(\gamma-1)}\} / \left\{ \left[ \frac{2}{\gamma-1} \right]^{1/2(\gamma-1)} [5(1 - \cos \theta_m)]^{1/2} \left[ \cos^{-1/2} \left( \frac{\pi}{2} \frac{\theta}{\theta_m} \right) + K \sin^n \left( \frac{\pi}{2} \frac{\theta}{\theta_m} \right) \right]^{1/(\gamma-1)} \right\} \quad (9)$$

Noting again that at large distances from the nozzle the streamlines appear to be straight radial lines emanating from a point source, the streamwise expansion is assumed to be nearly one-dimensional. This assumption provides the basic criteria for shaping the property contours. From continuity and one-dimensional momentum, the area ratio and Mach number can be expressed as<sup>4</sup>

$$\frac{A}{A^*} = \frac{1}{M} \left[ \frac{2}{\gamma+1} \left( 1 + \frac{\gamma-1}{2} M^2 \right) \right]^{(\gamma+1)/2(\gamma-1)} \quad (10)$$

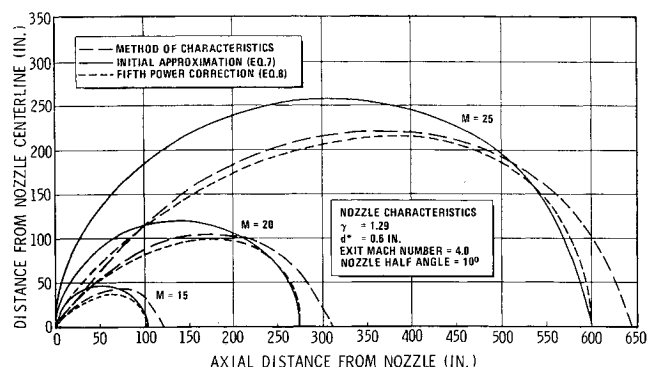


Fig. 2 Comparison of Mach contours obtained by method-of-characteristics and approximate solutions.

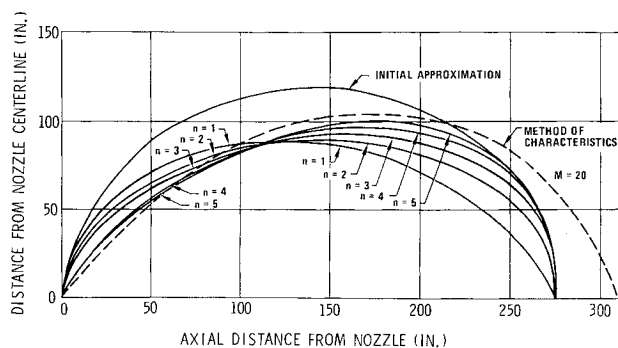


Fig. 3 Effect of the shaping term exponent  $n$  on the shape of the Mach contour.

At large  $r$ ,  $[(\gamma - 1)/2]M^2 \gg 1$ , and Eq. (10) becomes

$$A/A^* = M^{2/\gamma-1} [(\gamma - 1)/(\gamma + 1)]^{(\gamma+1)/2(\gamma-1)} \quad (11)$$

Equation (11) expresses the expansion ratio from the nozzle throat to a particular property contour. Note that  $A$  is the area normal to the flow direction between any two adjacent streamlines and not the area along the property contour. For axisymmetric nozzles, these incremental areas are surfaces of revolution, whose sum along the entire contour is also given by

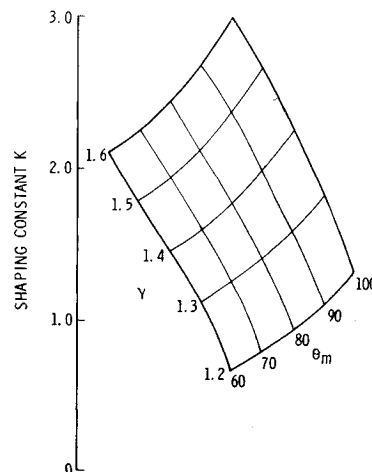
$$A = 2\pi \int_0^{\theta_m} r^2 \sin \theta d\theta \quad (12)$$

Equating the two area expressions given by Eqs. (11) and (12) and using Eq. (9) for  $r$  yields an integral equation for the two new constants  $K$  and  $n$  in terms of only the flow variables

$$\begin{aligned} &\gamma \text{ and } \theta_m. \text{ Thus} \\ &\int_0^{\theta_m} \left[ \cos^{-1/2} \left( \frac{\pi}{2} \frac{\theta}{\theta_m} \right) + K \sin^n \left( \frac{\pi}{2} \frac{\theta}{\theta_m} \right) \right]^{2/(1-\gamma)} \sin \theta d\theta \\ &= \frac{5}{8} \left( \frac{\gamma-1}{\gamma+1} \right)^{(\gamma+1)/2(\gamma-1)} \left( \frac{2}{(\gamma-1)} \right)^{1/(\gamma-1)} (1 - \cos \theta_m) \end{aligned} \quad (13)$$

Since  $\gamma$  and  $\theta_m$  are specified by the gas properties and the nozzle geometry,  $K$  is uniquely defined by the choice of the exponent  $n$ . Therefore, choosing  $n$  as an arbitrary constant fixes  $K$  for each nozzle geometry.

Fig. 4 Plume iso-Mach contour shaping constant for  $n = 5$ .



Limited calculations have been performed to determine the optimum value for the shaping term exponent. Figure 3 illustrates the effect of varying  $n$  from 1.0 to 5.0. Increasing this value generally tends to improve the approximation. However, a value of  $n = 5.0$  was found to be sufficiently accurate for most engineering approximations. Values of  $K$  were determined by a numerical scheme which solved for  $K$  by a combined iteration and integration of Eq. (13). A plot of the parameter for  $n = 5$  is presented in Fig. 4 as a function of  $\gamma$  and  $\theta_m$ . Figure 4, together with Eq. (6) and (8), define completely the constant property contours.

### Conclusions

By using the improved approximation as presently defined, the match with method-of-characteristics is achieved with sufficient accuracy everywhere except near the axis, although, as shown in Fig. 2, the percentage error improves with distance from the nozzle. This is due to the inaccuracy associated with Eq. (6), which thus far has been unaltered. Further improvement can be obtained by modifying the expressions for  $M_0$  (and all subsequent equations) in specific cases where some experimental (or reliable method-of-characteristics) data are available. Also, while the present scheme appears to yield quite acceptable answers for  $n = 5$ , it is readily adaptable to any other suitable value of  $n$ , provided that

new  $K$  values are computed consistent with the choice of the exponent  $n$ .

The clear-cut advantage of the scheme over those already available<sup>1,5</sup> is the extreme simplicity with which the complete flowfield (at large distances) can be approximated having only minimal nozzle dimensions and  $\gamma$ . It must be realized that the system is intended only as a means of rapid approximation; it is, therefore, limited (just as others are) to constant  $\gamma$ . Use of the technique for approximating reacting flows is possible provided that a suitable  $\gamma$  can be defined.

### References

- <sup>1</sup> Hill, J. A. F. and Draper, J. S., "Analytical Approximation For the Flow From a Nozzle into a Vacuum," *Journal of Spacecraft and Rockets*, Vol. 3, No. 10, Oct. 1966, pp. 1552-1554.
- <sup>2</sup> Sibulkin, M. and Gallaher, W. H., "Far Field Approximation for a Nozzle Exhausting into a Vacuum," *AIAA Journal*, Vol. 1, No. 6, June 1963, pp. 1452-1453.
- <sup>3</sup> Albini, F. A., "Approximate Computation of Underexpanded Jet Structure," *AIAA Journal*, Vol. 3, No. 6, Aug. 1965, pp. 1535-1537.
- <sup>4</sup> Owczarek, J. A., *Fundamentals of Gas Dynamics*, International Textbook Co., Scranton, Pa., 1964, pp. 200-206.
- <sup>5</sup> Brook, J. W., "Far Field Approximation for a Nozzle Exhausting into a Vacuum," *Journal of Spacecraft and Rockets*, Vol. 6, No. 5, May 1969, pp. 626-628.